A multi-layer functional genomic analysis to understand noncoding genetic variation in lipids

Ramdas, S., Judd, J., Graham, S. E., Kanoni, S., Wang, Y., Surakka, I., Wenz, B., Clarke, S. L., Chesi, A., Wells, A., Bhatti, K. F., Vedantam, S., Winkler, T. W., Locke, A. E., Marouli, E., Zajac, G. J. M., Wu, K.-H. H., Ntalla, I., Hui, Q., ... Million Veterans Program (2022). A multi-layer functional genomic analysis to understand noncoding genetic variation in lipids. *The American Journal of Human Genetics*, *109*(8), 1366-1387. https://doi.org/10.1016/j.ajhg.2022.06.012

Published in:
The American Journal of Human Genetics

Document Version:
Peer reviewed version

A multi-layer functional genomic analysis to understand noncoding genetic variation in lipids

Shweta Ramdas*, Jonathan Judd*, Sarah E Graham*, Stavroula Kanoni*, et al.

*equal contribution (co-first authors)

Corresponding Authors:

Xiang Zhu, PhD

Department of Statistics

Huck Institutes of the Life Sciences

The Pennsylvania State University

University Park, PA 16802

xiangzhu@psu.edu

Christopher D Brown, PhD

Department of Genetics

Perelman School of Medicine

University of Pennsylvania

Philadelphia PA 19104

chrbro@upenn.edu

Abstract

A major challenge of genome-wide association studies (GWAS) is to move from phenotypic associations to biological insight. Here, we integrate a large trans-ancestry GWAS on blood lipids with a wide array of functional genomic datasets to discover regulatory mechanisms underlying lipid associations. We first identify lipid-associated genes with expression quantitative trait locus - colocalizations, and then add chromatin interaction data to narrow the search for functional genes. Polygenic enrichment analysis across tissues and cell types confirms the central role of the liver in lipids, and highlights the selective enrichment of adipose-specific chromatin marks in high-density cholesterol and triglycerides. Overlapping transcription factor (TF) binding sites with lipid-associated loci, we identify TFs relevant in lipid biology. Finally, we present an integrative framework to prioritize causal variants at GWAS loci, producing a comprehensive list of candidate causal genes and variants with multiple layers of functional evidence. Two prioritized genes, *CREBRF* and *RRBP1,* show convergent evidence across functional datasets supporting their roles in lipid biology.

Introduction

Most GWAS findings have not directly led to mechanistic interpretations, largely because 90% of GWAS associations map to non-coding sequences [1,2]. Mechanistic interpretations in GWAS have proven challenging because the strongest signals identified in GWAS typically contain many variants in strong linkage disequilibrium (LD) [3] and functional mechanisms including genes of action are often not clear from GWAS data alone [4].

Linking trait-associated variants to genome function has emerged as a promising model for mechanistic interpretation of non-coding findings in GWAS. This 'variant-to-function' model is premised on recent observations that non-coding variants often affect a trait of interest through the regulation of genes and processes in trait-relevant cell types or tissues [2]. Implementing this functional model in GWAS has become more feasible as large-scale functional genomic resources, such as epigenomic [5,6] and transcriptomic catalogues [5] have been systematically generated across a wide range of human cell types and tissues. Indeed, the integration of functional genomics with GWAS has identified regulatory mechanisms in variants associated with obesity [7] and schizophrenia [8], yielding important functional insights in genetic architecture of human complex traits.

The history of the human genetics of lipids mirrors the success and challenge of GWAS. Increasing sample size and genetic diversity has significantly boosted the power of discovery: the first lipid GWAS in 2008 with 8,816 European-descent individuals

identified 29 lipid-associated loci[9] ; the latest study of 1.6 million individuals across five ancestries [Graham et al 2021] found 941. Despite the dramatic increase in the number of associations, our biological understanding of many of these genetic discoveries remains limited. The causal gene has been confidently assigned at only a small fraction of these loci [2], and the regulatory mechanism connecting variant to phenotype has been conclusively characterized only for a handful of genes [10]. Furthermore, systematic mapping of lipid-associated variants to their biological functions has been missing in literature at the time of this study.

Here we conduct a genome-scale integrative analysis on the largest GWAS to-date of five lipid phenotypes (LDL, or low density cholesterol; HDL, or high density cholesterol; TC, or total cholesterol; nonHDL, or non-high density cholesterol; and TG, or triglycerides) involving 1.6 million individuals from five ancestries [Graham et al 2021]. Combining the lipid GWAS with a wide array of functional genomic resources in diverse human tissues and cell types, we identify regulatory mechanisms of noncoding genetic variation in lipids with a full suite of computational approaches. Further, we develop a generalizable framework to understand how tissue-specific gene regulation can explain GWAS findings, and demonstrate its real-world value on lipid-associated loci.

Results

Figure 1: Starting with GWAS summary statistics for five lipid phenotypes, we integrate these with eQTL and chromatin interaction data to identify potential genes mediating the GWAS association, and use epigenomic annotations from ChIP-seq and ATAC-seq data both to identify regulatory mechanisms at these loci, and to arrive at genome-level insights into lipid biology, such as tissue relevance.

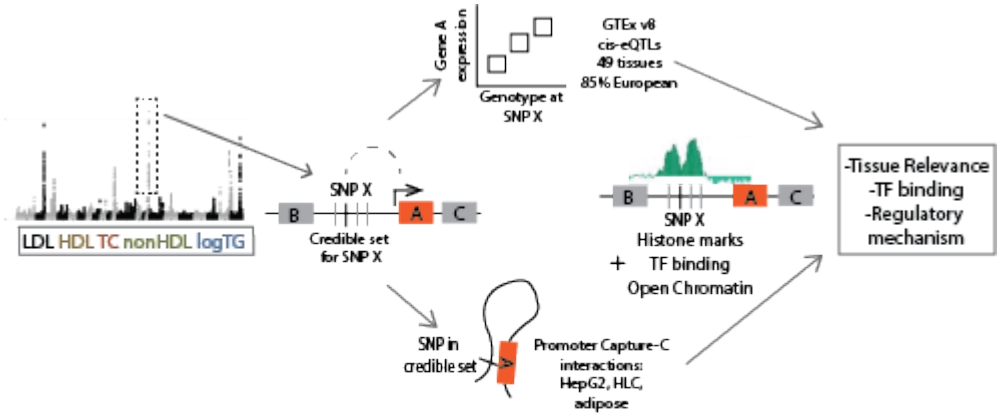

We systematically integrated lipid GWAS results [Graham et al 2021] with multiple layers of functional genomic data from diverse tissues and cell types to understand regulatory

mechanisms at lipid-associated loci (Figure 1). Specifically, we overlaid GWAS loci with expression quantitative trait loci (eQTL) and chromatin-chromatin interactions to identify causal genes. We further assessed polygenic enrichments of tissue-specific histone marks to prioritize relevant tissues and examined GWAS loci at transcription factor (TF) binding sites to detect lipid-relevant TFs. Finally, we combined all these layers to provide a holistic view of gene regulation at lipid loci in relevant tissue and cell types.

Co-localization with eQTLs identifies candidate lipid-relevant genes

We identify shared association signals between lipid levels and expression of nearby genes as a first step given that most GWAS signals are presumed to influence complex traits through their impact on gene expression [11]. To do so, we tested for colocalization of each of the significant lipid GWAS association signals (1,750 loci considering the five traits examined) with significant cis-eQTL data across 49 human tissues from the GTEx consortium [5]. Here, we defined GWAS signals as 1,750 loci reaching genome-wide significance and corrected for shadow signals (Methods) in a trans-ancestry meta-analysis for at least one of five lipid traits.

We then restricted our analysis to those loci likely mediated through regulatory mechanisms as opposed to coding variation. In particular, we excluded all loci with credible sets containing at least one missense variant (369 of 1,750 loci, 21% of credible sets (Paper2). Of the remaining 1,381 GWAS loci, 696 significantly colocalized with eQTLs (the ratio of posterior probability of a shared signal to the posterior probability of two signals being > 0.9 [12] ; Methods) in at least one of 49 tissues for at least one lipid phenotype. This resulted in 1,076 co-localized eGenes (an eGene is any gene with a significant eQTL as defined by GTEx); (range of 1 to 16 genes per locus; Table S1). Since with eQTL data alone it is difficult to disentangle a single functional gene from multiple functional (and likely coregulated) genes at a locus [13] we performed all downstream analyses with all 1,076 colocalized genes, to further prioritize functional genes at loci with multiple eGenes.

To acquire additional functional insights of colocalized genes, we assessed their enrichments across a wide range of existing biological and clinical gene sets. Colocalized genes showed enrichments in 20 KEGG pathways [14] at FDR 5% (Table S2), including known lipid-related processes such as cholesterol metabolism, PPAR signaling and bile secretion. These genes were enriched in 33 Mendelian genes from ClinVar [15] associated with lipid-related ICD codes (ICD code E78), (3.5 fold enrichment, including *APOB, LPL*, and *APOE*), suggesting the shared genetic basis of Mendelian and complex lipid phenotypes [16]. These genes were also enriched in 15 genes with rare-variant burden for lipid phenotypes from UK Biobank (11-fold enrichment, including genes *APOB, LPL, LIPG*

and *ANGPTL4*; Figure 2), confirming shared mechanisms of rare and common variation underlying lipid traits[16,17]. Altogether the results demonstrate the biological relevance of candidate functional genes prioritized by our approach.

Figure 2: Enrichment of eQTL/Capture-C overlap, and enrichment in 33 ClinVar gold standard genes. A. Numbers of genes identified by two approaches: eqtl colocalization (top panel) and promoter capture-c interactions (bottom panel) B. The intersection of eQTL and Capture-C datasets shows an enrichment beyond what is expected by chance, assuming both genesets are independent. C. The overlap between our list of prioritized genes with three sets of genes previously associated with lipid biology. Capture-C prioritized genes (on the left) show no enrichment, whereas colocalized genes (right) show a much higher overlap than expected by chance.

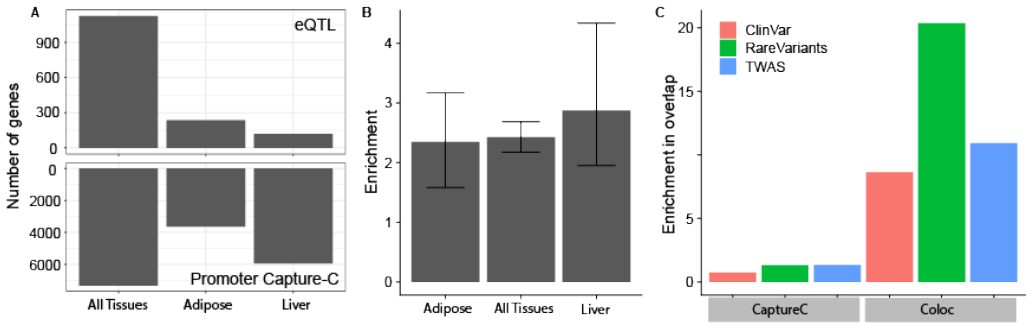

Chromatin-chromatin interactions improve eQTL-based colocalization

Our eQTL-based colocalization analysis uses a linear sequence of DNA, and ignores physical interaction between non-adjacent DNA segments, another regulatory layer underlying complex human traits [18]. To add this layer to our analysis, we generated promoter-focused Capture-C (henceforth called Capture-C) data from HepG2 liver carcinoma cells (denoted as HepG2.1) and hepatocyte-like cells (HLC) derived from differentiating iPSCs (the latter is described in [19]), as well as publicly-available Capture-C datasets from HepG2 [17,20] (denoted as HepG2.2) and adipose tissue [21]. We defined a GWAS-relevant interaction as any Capture-C interaction between any gene and the 95% credible set for a GWAS locus[22]. Credible set sizes ranged from 1 to 417 variants at the 1,750 examined loci, with a median size of 5 variants per credible set. In total, 1,079 GWAS loci had at least one variant in the credible set with a physical interaction with a gene promoter and 3,543 of 26,621 genes with promoter-interactions had promoters physically interacting with at least one GWAS credible set variant (Table S3). Unlike eQTL-colocalized genes, these genes interacting with their credible sets showed limited enrichment in relevant KEGG pathways and lipid-related genes from ClinVar (Figure 2B). We observed a similar lack of enrichment when we restricted the physical interaction analysis to protein-coding genes.

Genes physically interacting with GWAS loci helped shortlist functional genes from eQTL colocalization despite their lack of enrichments in known gene sets. Of 1,079 credible sets with promoter interactions, 224 also colocalized with eQTLs for the same gene (Figure 2A). Among these loci with concordant eQTL colocalizations and Capture-C interactions, only 39% of them mapped to a single gene using eQTL data alone, whereas adding Capture-C information increased this fraction to 80%. At the gene level, 233 genes were implicated in both eQTL colocalization and Capture-C interactions, representing an enrichment of 2.4. These results showcase the potential value of combining eQTLs with physical chromatin interactions to prioritize functional genes at GWAS loci.

Since eQTLs are likely to reside in the same TADs as the genes they regulate [23], we examined topologically associated domain (TAD) structure from independent datasets at lipids GWAS loci with eQTL colocalizations. Of eQTL-GWAS colocalizations in which the sentinel variant resided within a liver TAD [24], the colocalized gene resided in the same liver TAD 84.8% of the time (enrichment $P < 0.001$ with 1000 permutations; Methods). When we restricted colocalizations to those supported by Capture-C data in any cell type, 91.2% fall in the same TAD. These results add to the existing evidence for TAD boundaries being regulatory insulators in the cell [cite a recent review] and confirm our integration of chromatin interactions with eQTL colocalizations as an effective strategy to hone in on functional genes.

Tissue-specific enrichment of GWAS signals differentiates lipid traits

Regulatory variants often affect complex traits in a tissue-specific manner [25], as shown in our eQTL colocalization analysis. Specifically, by computing the ratio of the number of colocalizations in a tissue to eQTL sample size in that tissue, we identified that the liver was universally enriched for colocalized eGenes with respect to sample size across all lipid traits whereas adipose was selectively enriched in HDL and TG only (Figure S1). Motivated by these findings, we leveraged systematic approaches and additional data to identify relevant tissues and cell types for each lipid trait.

We implemented stratified LD score regression (S-LDSC), a polygenic approach not restricted only to genome-wide significant variants, on tissue-specific transcriptomic and epigenomic annotations to identify relevant tissues for each lipid trait (Methods). Consistent with previous studies and our eQTL-based analysis, liver-related tissues (tissue-groupings are defined in Table S4) showed strong enrichments across all lipid traits (S-LDSC enrichment p-values ranging from 1e-3 in TG to 1e-04 in TC), for both expression (Fig 3A) and chromatin annotations (Figure 3B). This result was further confirmed by two other approaches (DEPICT [26]: Figure S2; RSS-NET [27]: Table S5). To

assess the robustness of our S-LDSC results based on trans-ancestry GWAS data, we applied S-LDSC to two population-specific GWAS in GLGC (European and East Asian) together with population-specific LD scores (Methods), and we obtained similar results (Table S6).

Figure 3: Tissue relevance of lipid loci. Partitioning heritability of summary statistics on gene expression (top panel) and active regulatory marks (bottom panel) across tissues. Each plotted point represents each tested dataset for enrichment of heritability; multiple annotation datasets are tested for the same tissue group. Each color represents a single tissue group, and the y-axis represents P-value of enrichment of heritability. Liver-related tissues, in teal, consistently show strongest enrichment of heritability.

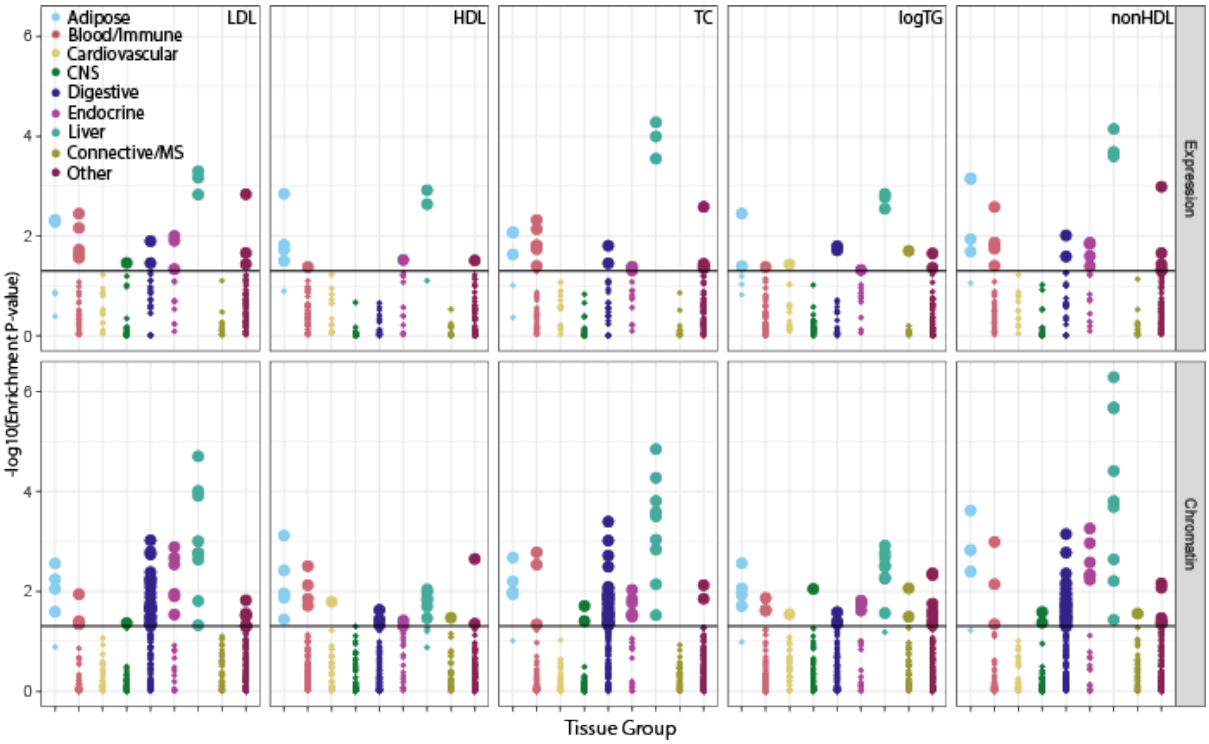

The S-LDSC results also highlighted tissues selectively enriched in certain lipid traits similar to the eQTL-based analysis. The most enriched category for HDL using chromatin annotation is 'Adipose H3K4me1'; for TG, enrichment in liver-related tissues is similar to enrichment in adipose. For LDL, TC and non-HDL, enrichment P-values for the liver were much more significant than for any other tissues (Figure 3B). We observed the same pattern in S-LDSC results based on gene expression (Figure 3A). This finding is consistent with the known influence of adipose on plasma HDL levels [28], and the role of adipose as TG deposits. These results were corroborated by eQTL colocalizations stratified by phenotype (Figure S1) and DEPICT analysis on gene expression [26] (Figure

S2). Together, these results strongly implicate the liver as the tissue of action for all five lipid traits, but additionally implicate adipose tissue as playing a role in HDL and TG.

Given the importance of the liver and adipose in modulating lipid levels, we further identified the relevant cell types within these tissues. Using published single-cell data from adipose and liver, we performed gene-set enrichment analysis [29] to identify cell-type clusters enriched for genes colocalized with any lipid trait. Out of 11 identified cell types in 20 clusters in the liver, only hepatocytes were enriched at $P < 0.05$ (Figure S3), consistent with previous results[20]. In adipose, only adipocyte clusters and macrophage-monocyte clusters showed suggestive enrichment in colocalized genes (Figure S4). Of note, the enrichment in adipocytes was significant when we restricted this analysis to genes that were colocalized only with HDL and TG (FDR-corrected $P < 0.05$), consistent with the selective enrichments of adipose in HDL and TG (but not the other lipid traits) from our S-LDSC analysis. Evaluations at cellular resolution are required to understand the cell-type specific mechanisms underlying lipid GWAS loci, but our results could form a useful basis for future studies.

Overlapping GWAS signals with binding sites highlights lipid-relevant TFs

TFs have been implicated as a key mediator of linking genetic variation to complex traits [30]. To understand lipid GWAS in the context of TF activity, we assessed enrichment of genome-wide significant variants at TF binding sites using GREGOR [31] and performed polygenic enrichment analysis of TF binding sites using S-LDSC.

Using ChIP-Seq data from 161 TFs across 91 cell types from the ENCODE project [6], 32.7% of lipid credible sets overlapped with at least one TF binding site. Using GREGOR [31], we identified 137 TFs whose binding sites were significantly enriched in GWAS lead SNPs for at least one lipid phenotype (enrichment > 2; FDR adjusted P-value < 0.05, Figure S5, Table S7). Among these 137 enriched TFs, 69 of them (50%) showed significant enrichments across all five lipid phenotypes, suggesting a potential core regulatory circuit shared by all lipid traits (Figure S5). The TF with the strongest enrichment in all phenotypes was *ESRRA* (Estrogen-related receptor alpha), a nuclear receptor active in metabolic tissues; ESRRA has been implicated in adipogenesis and lipid metabolism, and ESRRA-null mice display an increase in fat mass and obesity [32].

The GREGOR analysis also highlighted 68 TFs significantly enriched in specific subsets of (but not all five) lipid phenotypes (Figure S8). For example, we found 4 TFs (FOXM1, PBX3, ZKSCAN1, ZEB1) enriched in HDL and TG only, 4 TFs (EZH2, NFE2, NFATC1, KDM5A) enriched in HDL only and 11 TFs (FOSL1, IRF3, JUN, MEF2C, NANOG, PRDM1, RUNX3, SIRT6, SMC3, STAT3, ZNF217) enriched in TG only. Of these TFs, the central role

of *ZEB1* in adiposity [33] and fat cell differentiation has been demonstrated [34]. Taken together, these TF-centric findings corroborate the selective enrichments of adipose in HDL and TG (but not the other lipid traits) identified in our previous tissue prioritization analyses.

Similar to tissue prioritization, we also performed polygenic enrichment analysis of TF binding sites using S-LDSC (Table S8), which differed from GREGOR analysis by looking at not only the genome-wide significant associations but also the polygenic signal irrespective of GWAS P-values. On the same 161 ENCODE TFs, this polygenic analysis identified 25 TFs whose binding sites were significantly enriched in heritability for at least one lipid phenotype (Fig S6), and reassuringly, 24 of 25 TFs are also significant in GREGOR analysis. Among these enriched TFs, eight of them (34%) were significantly enriched in all five lipid traits (CEBPB, CEBPD, FOXA2, HDAC2, HNF4G, NFYA, RXRA, SP1; enrichment $P < 0.05$). Of those TFs significant in both analyses, Retinoid X receptor alpha (*RXRA*) is also a colocalized gene near a GWAS hit (chr9:137,268,682). *RXRA* is a ligand-activated transcription factor that forms heterodimers with other receptors (including *PPARG*) and is involved in lipid metabolism [35] and homeostasis. While *RXRA* has been implicated as the causal gene at its GWAS locus [36], our study is the first to demonstrate its role in lipid biology through its regulatory influence on other lipid GWAS genes.

Multi-layer functional integration reveals regulatory mechanisms at GWAS loci

Motivated by our finding that integrating chromatin interaction improved eQTL colocalizations, we further collated multiple lines of functional evidence at each GWAS locus for mechanistic inference. We started with the list of genes with evidence for both eQTL colocalization in the liver or adipose and credible set physical interactions. We next annotated each variant in the 95% credible set with various indicators of regulatory function, including its open chromatin status in liver or adipose-related cell types, its proximity to a promoter or an enhancer, and its RegulomeDB regulation probability [37] (see Table S9 for the complete list of annotations used). To account for complexities of regulatory mechanisms and limitations of functional datasets, we combined evidence across these datasets to prioritize variants at GWAS loci (Figure 4A). Specifically, we prioritized variants with at least three independent lines of functional evidence (chromatin openness, physically interaction with target genes, and promoter/enhancer status in liver or adipose), with at least two being in the same tissue with colocalization with the target gene, and with a RegulomeDB score > 0.5. Applying this simple procedure to lipid GWAS we identified 14 candidate loci, each with the strongest multi-layer evidence pointing to a single functional variant (Table 1). Below we used *RRBP1* and *CREBRF* to highlight key features of this multi-layer integration framework.

The first example *RRBP1* (Ribosomal binding protein 1) could be identified from eQTL colocalization alone, but our multi-layer integration approach strengthened the conclusion via convergent evidence from various sources (Figure 4B). The *RRBP1* eQTL signals in the liver colocalize with LDL, TC and nonHDL. The 'T' allele of the single lead variant (chr20:17,844,684, hg19) decreases *RRBP1* expression levels and increases LDL, TC and nonHDL levels. This lead variant at *RRBP1* is in open chromatin in HLC, and also physically interacts with the *RRBP1* promoter (250kb away) in adipose and HepG2. All these data based on the lead variant consistently point to *RRBP1* as the functional gene underlying this locus, which is further supported by external data. RRBP1 specifically tethers the endoplasmic reticulum to the mitochondria in the liver--an interaction that is enriched in hepatocytes--and regulates very low density lipoprotein (vLDL) levels [38]. Rare variants in *RRBP1* are associated with LDL in humans [39] and silencing *RRBP1* in liver affects lipid homeostasis in mice [38].

Figure 4. A. Variant annotation and prioritization scheme at each credible set. B. Evidence for gene RRBP1 from functional genomics data. The LDL GWAS locus at this region is an eQTL for gene RRBP1 in the liver (second panel). Variants in the credible set of this locus interact with the gene promoter in both adipose and HepG2 Capture-C data. The interacting variant is also in an open chromatin peak in three liver-related cell types. C. Multiple sources of functional genomics data support CREBRF as a gene contributing to HDL levels. The HDL GWAS locus at this region is an eQTL for gene CREBRF in Adipose (second panel). Variants in the credible set at this locus interact with the CREBRF promoter in adipose. The interacting variant is also in open chromatin in liver-related cell types.

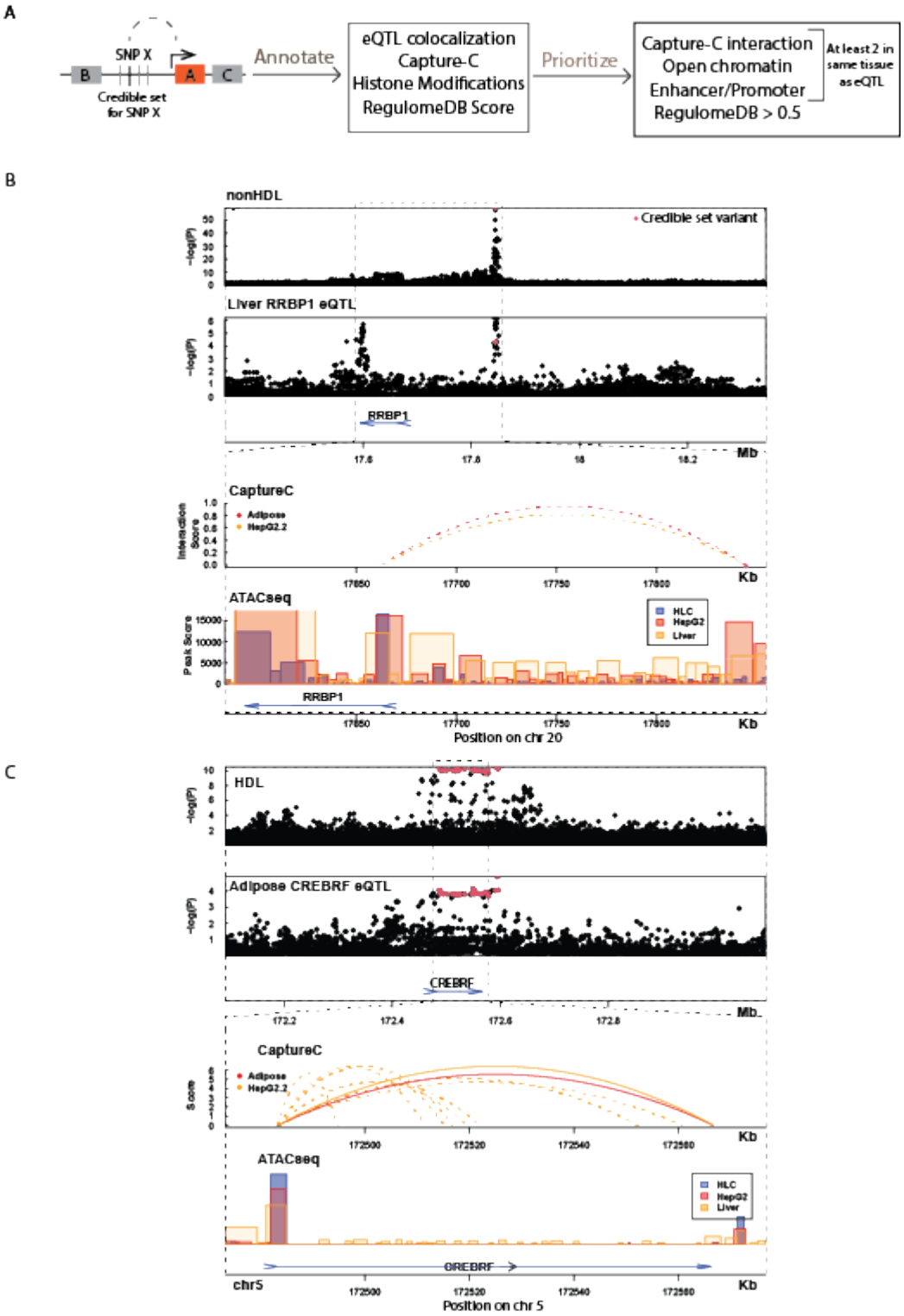

The second example *CREBRF* (CREB3 regulatory factor) demonstrates the power of our multi-layer integration framework in prioritizing functional variants (Figure 4C). The eQTL signals of *CREBRF* colocalized with a GWAS locus for HDL with 30 candidate variants. In contrast, our multi-layer approach identified a single candidate variant (chr5:172,566,698) at this locus that physically interacts with the *CREBRF* promoter in

adipose, was predicted to be a regulatory element (RegulomeDB score=0.91). Consistent with the index variant (chr5:172,591,337), the allele 'A' at this functional variant increased HDL levels and increased *CREBRF* expression in adipose. Missense variants in *CREBRF* have been linked to body mass index, and the gene has been linked to obesity risk in Samoans [40 41].

Discussion

Here we integrate the largest trans-ancestry lipid GWAS to date with a wide array of functional genomic resources to understand how noncoding genetic variation affects lipids through gene regulation. Specifically, we identify 1,076 genes whose eQTL signals colocalize with lipid GWAS signals and demonstrate how physical chromatin interaction can improve standard eQTL-based colocalization. We assess tissue-specific enrichments of lipid GWAS signals and demonstrate the selective importance of adipose in HDL and triglyceride biology. We examine binding site enrichments of 137 TFs in lipid GWAS and expand our understanding of lipid GWAS loci (e.g., *RXRA*) in the context of TF activity. Finally, we build a simple and interpretable prioritization framework that automatically combines multiple lines of evidence from orthogonal datasets, pinpointing a single functional variant at each of 14 lipid-associated loci (e.g., *RRBP1* and *CREBRF*). While there are studies that interpret lipid GWAS associations [20,42,43], the size of our trans-ancestry GWAS and multi-layer functional integration represent a comprehensive effort and an important step forward in this direction.

Our multi-layer analysis has two key strengths. First, despite a large array of functional genomic resources being embedded, our analysis produces results with high consistency. For example, the selective enrichment of adipose in HDL and TG identified by S-LDSC is confirmed by our eQTL-based colocalization and TF binding site overlap. Another example is the prioritization of *RRBP1*, which can be identified from eQTL-based colocalziation alone and it is further validated by chromatin openness and interaction. Such convergent evidence from various sources improves the confidence of our findings. Second, our analysis highlights that combining multiple layers of regulatory information can improve sensitivity to prioritize functional genes and variants. For example, we refined eQTL colocalized genes (1,076) to a smaller set of functional genes (233) through integration with promoter Capture-C data. Another example is *CREBRF*, where eQTL-based colocalization implicates 30 candidate variants and adding other regulatory layers points to a single functional variant. Moving forward, we expect these findings will serve as useful guidelines for future integrative genomic analyses of other traits.

Our results rely on the breadth and accuracy of functional genomic datasets used in our analyses. First, unlike our lipid GWAS, current functional datasets [44] are limited both in sample size and ancestral diversity, which can affect discovery and replication of regulatory mechanisms in diverse populations. Second, some functional datasets are generated at limited resolution. For example, our colocalizations are based on eQTLs from bulk tissue RNA-seq [5,45], which may miss detailed cell types and biological processes in which lipid-associated SNPs regulate gene expression [45]. Third, some functional datasets are not available across the full spectrum of human tissues and cell types. For example, our chromatin-chromatin interaction analysis only examines a few cell types in two known lipid-related tissues, producing results that may be biased towards known lipid biology. As more comprehensive and accurate functional genomic resources are becoming publicly available in diverse cellular contexts and ancestry groups, the resolution and power of integrative analyses like ours we applied here will be markedly increased.

Other limitations of this study stem from computational methods embedded in our framework. First, the colocalization approach 'coloc' assumes one causal variant per locus, whereas recent studies suggest extensive allelic heterogeneity [46] consistent with a model of a milieu of related transcription factors binding within a single locus. Accounting for allelic heterogeneity in summary statistics-based colocalization typically requires modeling of LD matrix [47], which is computationally intensive in large-scale analyses derived from many cohorts with diverse ancestries, like the trans-ancestry GWAS examined here. Second, due to restricted access to individual genotypes of 201 cohorts, we cannot produce trans-ethnic LD scores within GLGC but have to use European-based LD scores in all S-LDSC analyses. This approach, though less rigorous in principle, provides robust results in practice (as confirmed by our ancestry-specific analysis), largely because 79% of cohorts in GLGC are of European descent [Graham et al 2021]. That said, we caution that the same approach might fall short in ancestrally diverse studies with few European individuals [48]. Third, our multi-layer variant prioritization framework is built on a series of simple rules that are easy to implement on large datasets. This approach could possibly be formalized as statistical models (e.g., priors in Bayesian methods [27], but certainly simplify computation and improve scalability of our framework. Despite the technical limitations, our approach here can serve as a useful benchmark for future development of methods with improved statistical rigor and computation efficiency.

In summary, mapping noncoding genetic variation of complex traits to biological functions can benefit greatly from thorough integration of multiple layers of functional genomics, as demonstrated in the present study. Although tested on lipids only, our integrative framework is straightforward to implement more broadly on many other phenotypes, likely yielding functional insights of heritable traits and diseases in humans.

Methods

GWAS

We performed GWAS for five blood lipid traits (LDL, HDL, TC, TG, and nonHDL) in 1.65 million individuals from five ancestry groups \cite{Graham2021} (AFR: African and African-admixed; EAS: East Asian; EUR: European; HIS: Hispanic; SAS: South Asian; at 91 million variants imputed primarily from the Haplotype Reference Consortium or 1000 Genomes Phase 3. The individual GWAS and meta-analyses (described in Graham et al, 2021) were performed using the hg19 version of the human reference genome. We used MR-MEGA [49] for meta-analysis across cohorts.

We defined 'sentinel variants' as lead variants representing independent trait-associated loci in the genome. These windows are the greater of 500kb or 0.25cM around the sentinel variant; genetic distances were defined using reference maps from HapMap 3. We performed a second round of conditional analysis conditioning on the lead variants to identify and remove any significant windows that are actually shadow signals (or dependent on) of a neighboring locus to enforce true independence of associated loci.

Co-localization with gene expression

We performed statistical colocalization with eQTLs obtained from GTEx v8. These summary statistics were in GRCh38, so we first lifted over the GWAS summary statistics (in hg19) from the trans-ethnic summary statistics to GRCh38 using UCSC liftOver executable [50]. For each of the five lipid traits, we used the same 'sentinel variants' defined in the previous section to represent approximately independent GWAS-associated windows (also removing shadow signals as described before).

For each such window, we ran an eQTL colocalization using GTEx v8 eQTL summary statistics [5]. For each of 49 GTEx tissues, we first identified all genes within 1Mb of the sentinel SNP, and then restricted analysis to those genes with eQTLs ('eGenes') in that tissue (FDR < 0.05). We used the R package 'coloc' (run on R version 3.4.3, coloc version 3.2.1) [51] with default parameters to run co-localization between the GWAS signal and the eQTL signal for each of these cis-eGenes, using as input those SNPs in the defined

window, i.e. all SNPs present in both datasets. A colocalization posterior probability of (PP3+PP4) > 0.8 was used to identify loci with enough colocalization power, and PP4/PP3 > 0.9 was used to define those loci that show significant colocalization, described previously [12].

Overlap with promoter Capture-C data

We used four promoter Capture-C datasets from three cell/tissue types to capture physical interactions between gene promoters and their regulatory elements. We employed three biological replicates of HepG2 liver carcinoma cells [52], another HepG2 dataset described in Selvarajan et al [12,20], hepatocyte-like cells (HLC) produced by differentiating three biological replicates of iPSCs, which in turn were generated from peripheral blood mononuclear cells using a previously published protocol [19], and an adipose dataset obtained from Pan et al [21] that was produced using primary human white adipocytes.

The detailed protocol to prepare HepG2 or HLC cells for the promoter Capture-C experiment is described in [52]. Briefly, for each dataset, 10 million cells were used for promoter Capture-C library generation. Custom capture baits were designed using an Agilent SureSelect library design targeting both ends of DpnII restriction fragments encompassing promoters (including alternative promoters) of all human coding genes, noncoding RNA, antisense RNA, snRNA, miRNA, snoRNA, and lincRNA transcripts, totaling 36,691 RNA baited fragments shows the custom bait map boundaries in hg19 coordinates). Each library was then sequenced on an Illumina NovoSeq (HLC), or Illumina HiSeq 4000 (HLC), generating 1.6 billion read pairs per sample (50 base pair read length.) HiCUP [53] was used to process the raw FastQ files into loop calls; we then used CHiCAGO [53,54] to define significant looping interactions; a default score of 5 was defined as significant.

Starting with Capture-C maps processed as described above, we re-annotated the baits to gene IDs from Gencode v19 [55] to ensure uniformity of gene annotations with the rest of our pipeline. For each bait, we identified any gene whose transcription start site (TSS) from any transcript in Gencode v19 was within 175 base pair distance from the bait to account for differing bait designs for external datasets which may not directly overlap canonical TSS. From GRanges (version 1.42.0 run on R 4.0.2)[56], the findOverlaps function was used for this annotation with the 'maxgap' input set to 175. The final result annotated each bait to a unique gene name and Ensembl ID. The Ensembl IDs were formatted to remove the ID suffix, which included all numeric values after the ".". All datasets were additionally filtered to only include interactions in which the interacting end was not another bait.

Overlap between promoter Capture-C data and GWAS credible sets

To identify genetic variants associated with any of the five lipid traits that physically interact with locations in the genome that may influence lipid biology, we continued to use the R package 'Genomic Ranges' [56] to find overlap between previously defined credible sets for each traits' GWAS and the previously annotated promoter Capture-C data, which we refer as Capture-C/GWAS interactions. For all individual variants within all GWAS-associated loci for the five lipid traits, we identified which variants overlapped any interacting end of the four previously annotated promoter Capture-C data.

Enrichment of colocalized gene-sentinel variant pairs in topologically associated domains

To compute enrichment of colocalized gene-sentinel pairs in the same TAD, we used publicly-available TADs from the liver [24]. We compared the number of colocalizations with the sentinel variant and colocalized gene in the same TAD divided by all colocalizations in which the sentinel variant lies in a TAD.

Enrichment in single cell data from liver and adipose

We overlapped our list of colocalized genes with publicly available single cell RNA-sequencing data from cells in the liver [57] and 38,408 cells from the adipose [58]. For both datasets, we downloaded normalized TPM data and existing tSNE cluster annotations for each cell. For each cluster, we defined median expression for each gene across all cells in that cluster. Then for each cluster, we calculated the enrichment P-value for our list of colocalized genes using the 'fgsea' R package, which looks for overrepresentation of our gene list in ranked genes for each cluster [59], implemented in R 3.4.3.

Pathway Enrichment

We used ClusterProfiler v3.6.0 [60] to look for pathways over-represented in each gene list (genes with eQTL colocalization, and genes interacting with GWAS credible sets). Specifically, we used the enrichKEGG function to look for pathway enrichment in KEGG pathways. We first re-mapped gencode IDs to gene symbols using the Gencode v24 annotation and then used the biomaRt package [53,54,61] in R to convert gene symbols to Entrez IDs, and then ran enrichKEGG to identify enriched pathways significant at a Benjamini-Hochberg threshold of 0.05.

Stratified LD score regression for prioritizing tissues

We used LDSC version 1.0.1[62] to estimate the enrichment of heritability of our summary statistics in different epigenetic and transcriptomic annotations (including gene expression from GTEx, and histone epigenetic marks from Roadmap), using python 2.7.9. We first converted the summary statistics for each phenotype to LDSC-formatted summary statistics using 'munge_sumstats.py'. Then, we used 'ldsc.py' using the baseline_v1.2 baseline model and 'Multitissuechromatin1000Gv3' and 'Multitissuegeneexpr1000Gv3' annotations to estimate enrichment of heritability, using active chromatin marks and gene expression regularly. Links to downloaded files are in Supplementary Information. For primary analyses, we used trans-ethnic GWAS summary statistics, and ld scores from 1000Genomes European samples.

References

1. Gallagher, M.D., and Chen-Plotkin, A.S. (2018). The Post-GWAS Era: From Association to Function. Am. J. Hum. Genet. *102*, 717–730.

2. Cano-Gamez, E., and Trynka, G. (2020). From GWAS to Function: Using Functional Genomics to Identify the Mechanisms Underlying Complex Diseases. Front. Genet. *11*, 424.

3. Schaid, D.J., Chen, W., and Larson, N.B. (2018). From genome-wide associations to candidate causal variants by statistical fine-mapping. Nat. Rev. Genet. *19*, 491–504.

4. Smemo, S., Tena, J.J., Kim, K.-H., Gamazon, E.R., Sakabe, N.J., Gómez-Marín, C., Aneas, I., Credidio, F.L., Sobreira, D.R., Wasserman, N.F., et al. (2014). Obesity-associated variants within FTO form long-range functional connections with IRX3. Nature *507*, 371–375.

5. Consortium, T.G., and The GTEx Consortium (2020). The GTEx Consortium atlas of genetic regulatory effects across human tissues. Science *369*, 1318–1330.

6. ENCODE Project Consortium (2012). An integrated encyclopedia of DNA elements in the human genome. Nature *489*, 57–74.

7. Loos, R.J.F., and Yeo, G.S.H. (2021). The genetics of obesity: from discovery to biology. Nat. Rev. Genet.

8. Huo, Y., Li, S., Liu, J., Li, X., and Luo, X.-J. (2019). Functional genomics reveal gene regulatory mechanisms underlying schizophrenia risk. Nat. Commun. *10*, 1–19.

9. Willer, C.J., Sanna, S., Jackson, A.U., Scuteri, A., Bonnycastle, L.L., Clarke, R., Heath, S.C., Timpson, N.J., Najjar, S.S., Stringham, H.M., et al. (2008). Newly identified loci that influence lipid concentrations and risk of coronary artery disease. Nat. Genet. *40*, 161–169.

10. Musunuru, K., Strong, A., Frank-Kamenetsky, M., Lee, N.E., Ahfeldt, T., Sachs, K.V., Li,

X., Li, H., Kuperwasser, N., Ruda, V.M., et al. (2010). From noncoding variant to phenotype via SORT1 at the 1p13 cholesterol locus. Nature *466*, 714–719.

11. Neumeyer, S., Hemani, G., and Zeggini, E. (2020). Strengthening Causal Inference for Complex Disease Using Molecular Quantitative Trait Loci. Trends Mol. Med. *26*, 232–241.

12. Çalışkan, M., Manduchi, E., Rao, H.S., Segert, J.A., Beltrame, M.H., Trizzino, M., Park, Y., Baker, S.W., Chesi, A., Johnson, M.E., et al. (2019). Genetic and Epigenetic Fine Mapping of Complex Trait Associated Loci in the Human Liver. Am. J. Hum. Genet. *105*, 89–107.

13. (2014). Obesity and FTO: Changing Focus at a Complex Locus. Cell Metab. *20*, 710–718.

14. Kanehisa, M., Sato, Y., Kawashima, M., Furumichi, M., and Tanabe, M. (2016). KEGG as a reference resource for gene and protein annotation. Nucleic Acids Res. *44*, D457–D462.

15. Landrum, M.J., Chitipiralla, S., Brown, G.R., Chen, C., Gu, B., Hart, J., Hoffman, D., Jang, W., Kaur, K., Liu, C., et al. (2020). ClinVar: improvements to accessing data. Nucleic Acids Res. *48*, D835–D844.

16. Blair, D.R., Lyttle, C.S., Mortensen, J.M., Bearden, C.F., Jensen, A.B., Khiabanian, H., Melamed, R., Rabadan, R., Bernstam, E.V., Brunak, S., et al. (2013). A nondegenerate code of deleterious variants in Mendelian loci contributes to complex disease risk. Cell *155*,.

17. Teslovich, T.M., Musunuru, K., Smith, A.V., Edmondson, A.C., Stylianou, I.M., Koseki, M., Pirruccello, J.P., Ripatti, S., Chasman, D.I., Willer, C.J., et al. (2010). Biological, clinical and population relevance of 95 loci for blood lipids. Nature *466*, 707–713.

18. (2014). The 3D Genome in Transcriptional Regulation and Pluripotency. Cell Stem Cell *14*, 762–775.

19. Pashos, E.E., Park, Y., Wang, X., Raghavan, A., Yang, W., Abbey, D., Peters, D.T., Arbelaez, J., Hernandez, M., Kuperwasser, N., et al. (2017). Large, Diverse Population Cohorts of hiPSCs and Derived Hepatocyte-like Cells Reveal Functional Genetic Variation at Blood Lipid-Associated Loci. Cell Stem Cell *20*, 558–570.e10.

20. Selvarajan, I., Toropainen, A., Garske, K.M., López Rodríguez, M., Ko, A., Miao, Z., Kaminska, D., Õunap, K., Örd, T., Ravindran, A., et al. (2021). Integrative analysis of liver-specific non-coding regulatory SNPs associated with the risk of coronary artery disease. Am. J. Hum. Genet. *108*, 411–430.

21. Pan, D.Z., Garske, K.M., Alvarez, M., Bhagat, Y.V., Boocock, J., Nikkola, E., Miao, Z., Raulerson, C.K., Cantor, R.M., Civelek, M., et al. (2018). Integration of human adipocyte chromosomal interactions with adipose gene expression prioritizes obesity-related genes from GWAS. Nat. Commun. *9*, 1512.

22. Wakefield, J. (2009). Bayes factors for genome-wide association studies: comparison with P-values. Genet. Epidemiol. *33*, 79–86.

23. Yu, J., Hu, M., and Li, C. (2019). Joint analyses of multi-tissue Hi-C and eQTL data demonstrate close spatial proximity between eQTLs and their target genes. BMC Genet. *20*, 43.

24. Leung, D., Jung, I., Rajagopal, N., Schmitt, A., Selvaraj, S., Lee, A.Y., Yen, C.-A., Lin, S., Lin, Y., Qiu, Y., et al. (2015). Integrative analysis of haplotype-resolved epigenomes across human tissues. Nature *518*, 350–354.

25. Hekselman, I., and Yeger-Lotem, E. (2020). Mechanisms of tissue and cell-type specificity in heritable traits and diseases. Nat. Rev. Genet. *21*, 137–150.

26. Pers, T.H., Karjalainen, J.M., Chan, Y., Westra, H.-J., Wood, A.R., Yang, J., Lui, J.C., Vedantam, S., Gustafsson, S., Esko, T., et al. (2015). Biological interpretation of genome-wide association studies using predicted gene functions. Nat. Commun. *6*, 5890.

27. Zhu, X., Duren, Z., and Wong, W.H. (2021). Modeling regulatory network topology improves genome-wide analyses of complex human traits. Nat. Commun. *12*, 2851.

28. Zhang, T., Chen, J., Tang, X., Luo, Q., Xu, D., and Yu, B. (2019). Interaction between adipocytes and high-density lipoprotein:new insights into the mechanism of obesity-induced dyslipidemia and atherosclerosis. Lipids Health Dis. *18*, 223.

29. Subramanian, A., Tamayo, P., Mootha, V.K., Mukherjee, S., Ebert, B.L., Gillette, M.A., Paulovich, A., Pomeroy, S.L., Golub, T.R., Lander, E.S., et al. (2005). Gene set enrichment analysis: a knowledge-based approach for interpreting genome-wide expression profiles. Proc. Natl. Acad. Sci. U. S. A. *102*, 15545–15550.

30. Degtyareva, A.O., Antontseva, E.V., and Merkulova, T.I. (2021). Regulatory SNPs: Altered Transcription Factor Binding Sites Implicated in Complex Traits and Diseases. Int. J. Mol. Sci. *22*,.

31. Schmidt, E.M., Zhang, J., Zhou, W., Chen, J., Mohlke, K.L., Eugene Chen, Y., and Willer, C.J. (2015). GREGOR: evaluating global enrichment of trait-associated variants in epigenomic features using a systematic, data-driven approach. Bioinformatics *31*, 2601–2606.

32. Tripathi, M., Yen, P.M., and Singh, B.K. (2020). Estrogen-Related Receptor Alpha: An Under-Appreciated Potential Target for the Treatment of Metabolic Diseases. Int. J. Mol. Sci. *21*,.

33. Saykally, J.N., Dogan, S., Cleary, M.P., and Sanders, M.M. (2009). The ZEB1 Transcription Factor Is a Novel Repressor of Adiposity in Female Mice. PLoS One *4*, e8460.

34. Gubelmann, C., Schwalie, P.C., Raghav, S.K., Röder, E., Delessa, T., Kiehlmann, E., Waszak, S.M., Corsinotti, A., Udin, G., Holcombe, W., et al. (2014). Identification of the

652 transcription factor ZEB1 as a central component of the adipogenic gene regulatory
653 network. Elife *3*, e03346.

654 35. Neuschwander-Tetri, B.A. (2015). Retinoid X receptor: the forgotten partner in
655 regulating lipid metabolism? Am. J. Clin. Nutr. *102*, 5–6.

656 36. Willer, C.J., Schmidt, E.M., Sengupta, S., Peloso, G.M., Gustafsson, S., Kanoni, S.,
657 Ganna, A., Chen, J., Buchkovich, M.L., Mora, S., et al. (2013). Discovery and refinement of
658 loci associated with lipid levels. Nat. Genet. *45*, 1274–1283.

659 37. Boyle, A.P., Hong, E.L., Hariharan, M., Cheng, Y., Schaub, M.A., Kasowski, M.,
660 Karczewski, K.J., Park, J., Hitz, B.C., Weng, S., et al. (2012). Annotation of functional
661 variation in personal genomes using RegulomeDB. Genome Research *22*, 1790–1797.

662 38. Anastasia, I., Ilacqua, N., Raimondi, A., Lemieux, P., Ghandehari-Alavijeh, R., Faure, G.,
663 Mekhedov, S.L., Williams, K.J., Caicci, F., Valle, G., et al. (2021). Mitochondria-rough-ER
664 contacts in the liver regulate systemic lipid homeostasis. Cell Rep. *34*, 108873.

665 39. Jurgens, S.J., Choi, S.H., Morrill, V.N., Chaffin, M., Pirruccello, J.P., Halford, J.L., Weng,
666 L.-C., Nauffal, V., Roselli, C., Hall, A.W., et al. (2020). Rare Genetic Variation Underlying
667 Human Diseases and Traits: Results from 200,000 Individuals in the UK Biobank.

668 40. Loos, R.J.F. (2016). CREBRF variant increases obesity risk and protects against
669 diabetes in Samoans. Nat. Genet. *48*, 976–978.

670 41. Minster, R.L., Hawley, N.L., Su, C.-T., Sun, G., Kershaw, E.E., Cheng, H., Buhule, O.D.,
671 Lin, J., Reupena, M.S., Viali, S. 'itea, et al. (2016). A thrifty variant in CREBRF strongly
672 influences body mass index in Samoans. Nat. Genet. *48*, 1049–1054.

673 42. Klarin, D., Damrauer, S.M., Cho, K., Sun, Y.V., Teslovich, T.M., Honerlaw, J., Gagnon,
674 D.R., DuVall, S.L., Li, J., Peloso, G.M., et al. (2018). Genetics of blood lipids among
675 ~300,000 multi-ethnic participants of the Million Veteran Program. Nat. Genet. *50*, 1514–
676 1523.

677 43. Li, Z., Votava, J.A., Zajac, G.J.M., Nguyen, J.N., Leyva Jaimes, F.B., Ly, S.M., Brinkman,
678 J.A., De Giorgi, M., Kaul, S., Green, C.L., et al. (2020). Integrating Mouse and Human
679 Genetic Data to Move beyond GWAS and Identify Causal Genes in Cholesterol
680 Metabolism. Cell Metab. *31*, 741–754.e5.

681 44. Varshney, A., VanRenterghem, H., Orchard, P., Boyle, A.P., Stitzel, M.L., Ucar, D., and
682 Parker, S.C.J. (2019). Cell Specificity of Human Regulatory Annotations and Their Genetic
683 Effects on Gene Expression. Genetics *211*, 549–562.

684 45. van der Wijst, M.G.P., de Vries, D.H., Groot, H.E., Trynka, G., Hon, C.C., Bonder, M.J.,
685 Stegle, O., Nawijn, M.C., Idaghdour, Y., van der Harst, P., et al. (2020). Science Forum: The
686 single-cell eQTLGen consortium.

687 46. Arvanitis, M., Tayeb, K., Strober, B.J., and Battle, A. (2021). Redefining tissue
688 specificity of genetic regulation of gene expression in the presence of allelic

heterogeneity. medRxiv 2021.06.28.21259545.

47. Zhu, X., and Stephens, M. (2017). BAYESIAN LARGE-SCALE MULTIPLE REGRESSION WITH SUMMARY STATISTICS FROM GENOME-WIDE ASSOCIATION STUDIES. Ann. Appl. Stat. *11*, 1561–1592.

48. Wojcik, G.L., Graff, M., Nishimura, K.K., Tao, R., Haessler, J., Gignoux, C.R., Highland, H.M., Patel, Y.M., Sorokin, E.P., Avery, C.L., et al. (2019). Genetic analyses of diverse populations improves discovery for complex traits. Nature *570*, 514–518.

49. Mägi, R., Horikoshi, M., Sofer, T., Mahajan, A., Kitajima, H., Franceschini, N., McCarthy, M.I., COGENT-Kidney Consortium, T2D-GENES Consortium, and Morris, A.P. (2017). Trans-ethnic meta-regression of genome-wide association studies accounting for ancestry increases power for discovery and improves fine-mapping resolution. Hum. Mol. Genet. *26*, 3639–3650.

50. Kuhn, R.M., Haussler, D., and Kent, W.J. (2013). The UCSC genome browser and associated tools. Brief. Bioinform. *14*, 144–161.

51. Giambartolomei, C., Vukcevic, D., Schadt, E.E., Franke, L., Hingorani, A.D., Wallace, C., and Plagnol, V. (2014). Bayesian test for colocalisation between pairs of genetic association studies using summary statistics. PLoS Genet. *10*, e1004383.

52. Chesi, A., Wagley, Y., Johnson, M.E., Manduchi, E., Su, C., Lu, S., Leonard, M.E., Hodge, K.M., Pippin, J.A., Hankenson, K.D., et al. (2019). Genome-scale Capture C promoter interactions implicate effector genes at GWAS loci for bone mineral density. Nat. Commun. *10*, 1260.

53. Wingett, S., Ewels, P., Furlan-Magaril, M., Nagano, T., Schoenfelder, S., Fraser, P., and Andrews, S. (2015). HiCUP: pipeline for mapping and processing Hi-C data. F1000Res. *4*, 1310.

54. Cairns, J., Freire-Pritchett, P., Wingett, S.W., Várnai, C., Dimond, A., Plagnol, V., Zerbino, D., Schoenfelder, S., Javierre, B.-M., Osborne, C., et al. (2016). CHiCAGO: robust detection of DNA looping interactions in Capture Hi-C data. Genome Biol. *17*, 127.

55. Harrow, J., Frankish, A., Gonzalez, J.M., Tapanari, E., Diekhans, M., Kokocinski, F., Aken, B.L., Barrell, D., Zadissa, A., Searle, S., et al. (2012). GENCODE: the reference human genome annotation for The ENCODE Project. Genome Res. *22*, 1760–1774.

56. Lawrence, M., Huber, W., Pagès, H., Aboyoun, P., Carlson, M., Gentleman, R., Morgan, M.T., and Carey, V.J. (2013). Software for computing and annotating genomic ranges. PLoS Comput. Biol. *9*, e1003118.

57. MacParland, S.A., Liu, J.C., Ma, X.-Z., Innes, B.T., Bartczak, A.M., Gage, B.K., Manuel, J., Khuu, N., Echeverri, J., Linares, I., et al. (2018). Single cell RNA sequencing of human liver reveals distinct intrahepatic macrophage populations. Nat. Commun. *9*, 4383.

58. Single Cell Portal.

59. Korotkevich, G., Sukhov, V., Budin, N., Shpak, B., Artyomov, M.N., and Sergushichev, A. Fast gene set enrichment analysis.

60. Yu, G., Wang, L.-G., Han, Y., and He, Q.-Y. (2012). clusterProfiler: an R Package for Comparing Biological Themes Among Gene Clusters. OMICS: A Journal of Integrative Biology *16*, 284–287.

61. Durinck, S., Spellman, P.T., Birney, E., and Huber, W. (2009). Mapping identifiers for the integration of genomic datasets with the R/Bioconductor package biomaRt. Nat. Protoc. *4*, 1184–1191.

62. Finucane, A., Carduff, E., Meade, R., Doyle, S., Fenning, S., Cumming, S., Hekerem, D., Rahman, F., Lugton, J., Johnston, B., et al. (2021). Palliative care research promotion in policy and practice: a knowledge exchange process. BMJ Support. Palliat. Care.